LA-UR-84-3557

CONF-8411118--1

Los Alamos National Laboratory is operated by the University of California for the United States Department of Energy under contract W-7405-ENG-36.

TITLE: DIFFERENTIAL AND INTEGRAL COMPARISONS OF THREE REPRESENTATIONS OF THE PROMPT NEUTRON SPECTRUM FOR THE SPONTANEOUS FISSION OF ^{252}Cf.

AUTHOR(S): D(avid) G(eorge) Madland, T-2
R(aphael) J(oseph) LaBauve, T-2
J. R(ayford) Nix, T-9

LA-UR--84-3557

DE85 003728

SUBMITTED TO: THE ADVISORY GROUP MEETING ON NUCLEAR STANDARD REFERENCE DATA, GEEL, BELGIUM, NOVEMBER 12-16, 1984.

DISCLAIMER

Los Alamos National Laboratory
Los Alamos, New Mexico 87545

DIFFERENTIAL AND INTEGRAL COMPARISONS OF THREE REPRESENTATIONS OF THE PROMPT NEUTRON SPECTRUM FOR THE SPONTANEOUS FISSION OF ^{252}Cf

David G. Madland, Raphael J. LaBauve, and J. Rayford Nix

Theoretical Division
Los Alamos National Laboratory
Los Alamos, New Mexico 87545

November 1, 1984

ABSTRACT

Because of their importance as neutron standards, we present comparisons of measured and calculated prompt fission neutron spectra N(E) and average prompt neutron multiplicities $\bar{\nu}_p$ for the spontaneous fission of ^{252}Cf. In particular, we test three representations of N(E) against recent experimental measurements of the differential spectrum and threshold integral cross sections. These representations are the Maxwellian spectrum, the NBS spectrum, and the Los Alamos spectrum of Madland and Nix. For the Maxwellian spectrum, we obtain the value of the Maxwellian temperature T_M by a least-squares adjustment to the experimental differential spectrum of Poenitz and Tamura. For the Los Alamos spectrum, a similar least-squares adjustment determines the nuclear level-density parameter a, which is the single unknown parameter that appears. The NBS spectrum has been previously constructed by adjustments to eight differential spectra measured during the period 1965 to 1974. Among these three representations, we find that the Los Alamos spectrum best reproduces both the differential and integral measurements, assuming ENDF/B-V cross sections in the calculation of the latter. Although the NBS spectrum reproduces the integral measurements fairly well, it fails to satisfactorily reproduce the new differential measurement, and the Maxwellian spectrum fails to satisfactorily reproduce the integral measurements. Additionally, we calculate a value of $\bar{\nu}_p$ from the Los Alamos theory that is within approximately 1% of experiment.

I. INTRODUCTION

The prompt fission neutron spectrum N(E) and average prompt neutron multiplicity $\bar{\nu}_p$ from the spontaneous fission of ^{252}Cf are used as reference standards in the experimental and applied neutron physics fields. Accordingly, demand for improvement in the accuracy of these standards is constantly driven

by technical innovations and improvements that are occurring in these fields. For this reason we present detailed comparisons of recent measured and calculated prompt fission neutron spectra and average prompt neutron multiplicities for this standard reaction. In particular, we test three representations of N(E) against recent high-quality experimental measurements of the differential spectrum and threshold integral cross sections. These representations are the widely used Maxwellian spectrum, the National Bureau of Standards (NBS) spectrum,[1,2] and the Los Alamos spectrum based on the recent theory of Madland and Nix.[3-5]

For the Maxwellian spectrum, we obtain the value of the Maxwellian temperature T_M by a least-squares adjustment to the experimental differential spectrum of Poenitz and Tamura.[6,7] For the Los Alamos spectrum, a similar least-squares adjustment with respect to the same experimental spectrum determines the nuclear level-density parameter a, which is the single unknown parameter that appears. The NBS spectrum has been previously determined by empirical construction of line-segment corrections to a least-squares adjusted Maxwellian spectrum. Eight differential spectrum measurements from the period 1965 to 1974 were used in this determination.

Proceeding in three steps, we first present in Sec. II detailed descriptions of the physical content of the three spectrum representations to be tested. Second, in Sec. III we perform the least-squares adjustments of the Maxwellian and Los Alamos representations to the experimental differential spectrum of Poenitz and Tamura. We do not adjust the NBS representation since it has been previously determined. This is followed by a detailed comparison of the three spectra to the Poenitz and Tamura spectrum. We also compare in this section the value of $\bar{\nu}_p$ calculated with the Los Alamos theory to recent experimental values. Third, in Sec. IV we present fifteen integral cross-section calculations for each of the three spectrum representations and compare them with each other and with recent experimental integral cross sections as measured by Grundl et al.[8] and Kobayashi et al.[9,10] We present our conclusions from all comparisons in Sec. V.

II. THREE REPRESENTATIONS OF THE PROMPT FISSION NEUTRON SPECTRUM

In this section we describe the origin and physical content of the three representations of the prompt neutron spectrum for the spontaneous fission of ^{252}Cf that we are comparing in this work.

A. Maxwellian Spectrum.

The Maxwellian spectrum is given by

$$N(E) = \frac{2\sqrt{E}\ \exp(-E/T_M)}{\sqrt{\pi}\ T_M^{3/2}} \quad , \tag{1}$$

where E is the energy of the emitted neutron and T_M, the single parameter of the spectrum, is the Maxwellian temperature expressed in units of energy by absorption of the Boltzmann constant. Like all spectra considered in this work, this spectrum has units of inverse energy and is normalized to unity when integrated from zero to infinity. The mean and mean-square energy are given, respectively, by

$$\langle E \rangle = \frac{3}{2}\ T_M \quad , \text{ and} \tag{2}$$

$$\langle E^2 \rangle = \frac{15}{4}\ T_M^2 \quad . \tag{3}$$

The Maxwellian spectrum neglects the center-of-mass motion of the fission fragments from which the neutrons are emitted, the distribution of fission-fragment excitation energy, and the energy dependence of the inverse process to neutron emission, namely, compound nucleus formation. Accordingly, it has little physical basis for describing fission neutron spectra other than the correct energy dependence at both low and high energies.

Nevertheless, it has been widely used for this purpose, partly because of the convenience of a single parameter representation and partly for the following reason: In principle, the value of T_M must be rather large because T_M has to account not only for the average center-of-mass motion of the emitted neutrons, but also for the average center-of-mass motion of the fission fragments. In practice, however, the value of T_M is usually reduced in order that the spectrum reproduce the high-energy portion of the experimental spectrum. To preserve the normalization, this simultaneously increases the spectrum at lower energies, which then usually reproduces better the low-energy portion of the experimental spectrum. This spurious enhancement of energies below ~1 MeV simulates to some extent an effect that is due to the energy dependence of the cross section for the inverse process of compound nucleus formation, to be discussed later in this section. Thus, for the wrong physical reason, the Maxwellian spectrum reproduces a given experimental spectrum reasonably well, provided that the Maxwellian temperature T_M is suitably adjusted.

B. NBS Spectrum.

The NBS spectrum[1,2] is an empirically constructed spectrum that is based upon eight differential spectrum measurements performed during the period 1965 to 1974. The spectrum consists of a five-segment piecewise continuous representation containing twelve parameters and is given by

$$N(E) = \sum_{i=1}^{5} \mu_i(E)\, M(E) \quad , \tag{4}$$

where M(E) is the reference Maxwellian spectrum

$$M(E) = 0.6672 \sqrt{E} \exp(-E/1.42) \tag{5}$$

and $\mu_i(E)$ are five line-segment corrections given by

$$\begin{aligned}
\mu_1(E) &= 1 + 1.20E - 0.237, && 0 \leq E \leq 0.25 \text{ MeV}, \\
\mu_2(E) &= 1 - 0.14E + 0.098, && 0.25 \leq E \leq 0.8 \text{ MeV}, \\
\mu_3(E) &= 1 + 0.024E - 0.0332, && 0.8 \leq E \leq 1.5 \text{ MeV}, \\
\mu_4(E) &= 1 - 0.0006E + 0.0037, && 1.5 \leq E \leq 6.0 \text{ MeV, and} \\
\mu_5(E) &= \exp[-0.03(E - 6.0)], && 6.0 \leq E < \infty \quad .
\end{aligned} \tag{6}$$

In these equations, E is in units of MeV and N(E) is in units of MeV^{-1}. The mean and mean-square energy of the NBS spectrum, obtained by numerical integration, are given, respectively, by

$$\langle E \rangle = 2.120 \text{ MeV, and} \tag{7}$$

$$\langle E^2 \rangle = 7.433 \text{ MeV}^2 \quad . \tag{8}$$

The NBS spectrum was constructed by first obtaining a reference Maxwellian spectrum M(E) from a weighted least-squares adjustment to eight measured differential spectra, and second, by obtaining five line-segment corrections in a final adjustment to the same measurements. The temperature parameter of the reference Maxwellian has the value $T_M = 1.42$ MeV, corresponding to a mean energy $\langle E \rangle = 2.130$ MeV, which is 10 keV larger than the mean energy of the final spectrum. The difference is due largely to the influence of the exponential correction $\mu_5(E)$, which reduces slightly the high-energy portion of the reference Maxwellian M(E). In other words, the final adjustment in the NBS spectrum determined that the high-energy portion of the best-fit reference

Maxwellian was still somewhat larger than experiment. At the low-energy end of the final adjusted spectrum, the linear corrections $\mu_1(E)$ and $\mu_2(E)$ indicate that the best-fit reference Maxwellian is, again, slightly larger than experiment for very low energies, but near 0.25 MeV is somewhat less than experiment. Thus, the NBS spectrum differs from a best-fit Maxwellian spectrum primarily by a reduction from that spectrum at very low and high energies and by an enhancement to that spectrum at energies near 0.25 MeV. The consequences of these differences will become evident in Secs. III and IV.

C. Los Alamos Spectrum.

The Los Alamos theory is directed at predicting N(E) and $\bar{\nu}_p$ as functions of both the fissioning nucleus and its excitation energy.[3] The formalism is based upon standard nuclear evaporation theory and accounts for the physical effects of (1) the center-of-mass motion of the fission fragments, (2) the distribution of fission-fragment excitation energy, and (3) the energy dependence of the cross section for the inverse process of compound nucleus formation. The expression for the Los Alamos spectrum is given by the average of the spectra calculated for neutron emission from the light L and heavy H average fission fragments, namely

$$N(E) = \frac{1}{2}[N(E,E_f^L,\sigma_c^L) + N(E,E_f^H,\sigma_c^H)] \quad , \tag{9}$$

where E is the energy of the emitted neutron, E_f is the average kinetic energy per nucleon of a moving fission fragment, and σ_c is the compound nucleus formation cross section. The spectrum due to a moving fission fragment is given by

$$N(E,E_f,\sigma_c) = \frac{1}{2\sqrt{E_f}T_m^2} \int_{(\sqrt{E}-\sqrt{E_f})^2}^{(\sqrt{E}+\sqrt{E_f})^2} \sigma_c(\varepsilon)\sqrt{\varepsilon}\, d\varepsilon \times \int_0^{T_m} k(T)\, T \exp(-\varepsilon/T) dT \quad . \tag{10}$$

In this equation ε is the center-of-mass neutron energy, T is the fission-fragment residual nuclear temperature with a maximum value T_m, and k(T) is the temperature-dependent normalization constant for the corresponding center-of-mass spectrum.

The spectrum given by Eqs. (9) and (10) depends upon E_f^L, E_f^H, T_m, and the compound nucleus formation cross sections σ_c^L and σ_c^H, which are calculated by use of an optical-model potential. In this work we use the potential of Becchetti and Greenlees[11] to calculate these cross sections. The spectrum is evaluated numerically by Gaussian quadrature, as are its energy moments given by

$$\langle E^n \rangle = \int_0^\infty E^n \, N(E) dE \quad . \tag{11}$$

The values of E_f^L and E_f^H are obtained by use of momentum conservation, namely,

$$E_f^L = \frac{\langle A_H \rangle}{\langle A_L \rangle} \frac{\langle E_f^{tot} \rangle}{A} \quad , \text{ and} \tag{12}$$

$$E_f^H = \frac{\langle A_L \rangle}{\langle A_H \rangle} \frac{\langle E_f^{tot} \rangle}{A} \quad , \text{ where} \tag{13}$$

$\langle E_f^{tot} \rangle$ is the total average fission-fragment kinetic energy, A is the mass number of the compound nucleus undergoing fission, and $\langle A_L \rangle$ and $\langle A_H \rangle$ are the average mass numbers of the light and heavy fragments, respectively. For the spontaneous fission of ^{252}Cf, we use the values $\langle E_f^{tot} \rangle$ = 185.9 ± 0.5 MeV, $\langle A_L \rangle$ = 108, and $\langle A_H \rangle$ = 144 that are obtained from the measurements of Unik et al.[12]

The value of T_m is obtained from the initial total average fission-fragment excitation energy $\langle E^* \rangle$ by use of the relationship[13]

$$T_m = (\langle E^* \rangle / a)^{1/2} \quad , \tag{14}$$

where a is the nuclear level-density parameter. For spontaneous fission, $\langle E^* \rangle$ is given by

$$\langle E^* \rangle = \langle E_r \rangle - \langle E_f^{tot} \rangle \quad , \tag{15}$$

where $\langle E_r \rangle$ is the average energy release in fission. It is given exactly by

$$\langle E_r \rangle = \frac{\sum_{A_H} Y(A_H) E_r(A_H)}{\sum_{A_H} Y(A_H)} \quad , \tag{16}$$

where $Y(A_H)$ is the fission-fragment mass yield distribution, A_H is the heavy fragment mass number, and $E_r(A_H)$ is the average energy release for a given mass division. The latter quantity is obtained, in turn, by summing the contributions from all participating charge divisions, namely

$$E_r(A_H) = \frac{\sum_{Z_H} \rho(Z_H,A_H) E_r(Z_H,A_H)}{\sum_{Z_H} \rho(Z_H,A_H)} \quad , \tag{17}$$

where $\rho(Z_H,A_H)$ is the heavy fission-fragment charge distribution, Z_H is the heavy fragment atomic number, and $E_r(Z_H,A_H)$ is the energy release for a given mass and charge division. We assume the fission-fragment charge distribution to be of Gaussian form

$$\rho(Z_H,A_H) = \frac{1}{(2\pi\sigma_z^2)^{\frac{1}{2}}} \exp[-(Z_H - Z_H^P)^2/(2\sigma_z^2)] \quad , \tag{18}$$

with the most probable heavy fragment charge Z_H^P given by the relation

$$\frac{Z_H^P + c}{A_H} = \frac{Z}{A} = \frac{Z_L^P - c}{A_L} \quad , \tag{19}$$

where c is the charge division parameter.

For the spontaneous fission of ^{252}Cf we evaluate Eqs. (14)-(19) using experimental or derived systematic masses from the 1981 Wapstra-Bos evaluation[14] when they exist and otherwise the mass formula of Möller and Nix.[15] We use the fission-fragment mass-yield distribution $Y(A_H)$ measured by Weber et al.[16] and the value 0.5 charge units determined by Unik et al.[12] for the charge division parameter c, except for symmetric fission where c = 0. We also use a value of 0.5 charge units for the charge distribution width σ_z, which is approximately mid-range in the set of values determined by Wahl.[17] With these choices of mass sources, measured yields, and charge distribution parameters, we obtain a value for $\langle E_r \rangle$ of 218.886 MeV. This result was previously obtained in Ref.

4 and was used in Refs. 5 and 18. It is stable to within ± 55 keV for a change of ± 0.05 charge units in c and to within ± 220 keV for a change of ± 0.1 charge units in σ_z. These ranges are representative of the accuracy with which c and σ_z are known for the spontaneous fission of ^{252}Cf.

From Eqs. (14) and (15) we now obtain

$$T_m = (32.986/a)^{1/2} \text{ MeV}, \tag{20}$$

where the nuclear level-density parameter a is the single remaining parameter to be determined prior to calculating the spectrum. The determination of the level-density parameter and consequent calculation of the Los Alamos spectrum are presented in the next section. We will come back to Eq. (20) there.

Turning to the average prompt neutron mulitplicity, $\bar{\nu}_p$, the formalism for the Los Alamos spectrum gives[3]

$$\bar{\nu}_p = \frac{\langle E^* \rangle - \langle E_\gamma^{tot} \rangle}{\langle S_n \rangle + \langle \varepsilon \rangle} , \tag{21}$$

where $\langle E_\gamma^{tot} \rangle$ is the measured total average prompt gamma energy, $\langle S_n \rangle$ is the average fission-fragment neutron separation energy calculated in the same way as $\langle E_r \rangle$, and $\langle \varepsilon \rangle$ is the average center-of-mass energy of the emitted neutrons calculated in an analogous way to the average laboratory energy $\langle E \rangle$ from Eq. (11). For ^{252}Cf(sf) we obtain $\langle S_n \rangle$ = 5.439 MeV, a result previously obtained in Ref. 4 and utilized in Ref. 5. We obtain the value $\langle E_\gamma^{tot} \rangle$ = 7.06 MeV from the experiment of Pleasonton et al.[19] Using these values in Eq. (21), we obtain

$$\bar{\nu}_p = \frac{25.926 \text{ MeV}}{5.439 \text{ MeV} + \langle \varepsilon \rangle} , \tag{22}$$

where the evaluation of the average center-of-mass energy $\langle \varepsilon \rangle$ depends upon the evaluation of T_m, as given by Eq. (20). Accordingly, we return to Eq. (22) and the calculation of $\bar{\nu}_p$ in the next section.

III. DIFFERENTIAL COMPARISONS

In this section we compare the three representations of the prompt fission neutron spectrum that we are studying to each other and to a recent high-quality differential measurement of the spectrum. In fact, because of the use of the $^{252}Cf(sf)$ spectrum as a standard, we determine the Maxwellian temperature T_M by a least-squares adjustment to the experimental spectrum instead of by other means and, for the identical reason, we determine the nuclear level-density parameter a for the Los Alamos spectrum in the same way. The NBS spectrum, with twelve parameters, has been previously obtained by least-squares adjustments and therefore is already completely determined.

For our present purposes, we choose the recent differential spectrum measurement of Poenitz and Tamura[6,7] as our experimental reference spectrum. This experiment covers a secondary neutron energy range of 0.225 to 9.8 MeV with 51 points that represent approximately 95% of the total spectrum. The average experimental uncertainty in the set of 51 points is 3.6%.

A. Maxwellian Spectrum.

The least-squares adjustment of the Maxwellian spectrum to the experimental reference spectrum is performed with respect to the Maxwellian temperature parameter T_M. To obtain an absolute value of χ^2 per degree of freedom, the normalization of the experiment is recomputed for each iteration in the value of T_M. We find a minimum in χ^2, $\chi^2(\text{min}) = 1.201$, at a value of $T_M = 1.429$ MeV. This value yields mean and mean-square energies of the Maxwellian spectrum, from Eqs. (2) and (3), of 2.144 MeV and 7.658 MeV^2, respectively. These values are also given in Table I together with other properties of the Maxwellian spectrum.

The spectrum is computed using Eq. (1) and is compared to the experimental spectrum in Fig. 1 in absolute units, as well as in Figs. 2 and 3 where the ratio of the experimental spectrum to this spectrum is plotted. The highest energy experimental points on Fig. 1 indicate that perhaps the Maxwellian spectrum is slightly larger than experiment in this region. Inspection of Figs. 2 and 3 confirm this for energies greater than about 5 MeV, with departures from experiment that are perhaps as large as 10%. In addition, one sees

that the Maxwellian spectrum is larger than experiment by 2-7% in the region below 0.4 MeV and that it is smaller by 2-5% in the region between 1.5 and 3.0 MeV. Thus, the spurious enhancement in the Maxwellian spectrum at low energies that we discussed in Sec. II.A is apparently too large at energies below 0.4 MeV. At high energy, despite the adjustment of T_M with respect to experiment, the Maxwellian spectrum is still somewhat greater than experiment, reflecting the fundamental difficulty that we discussed in Sec. II.A in accounting for two physical effects with a single parameter.

B. NBS Spectrum.

The NBS spectrum is calculated using Eqs. (4)-(6). The comparison of this spectrum to the experimental differential spectrum is shown in Fig. 1 in absolute units, and in Fig. 2, where the ratios of this spectrum and the experimental spectrum to the least-squares adjusted Maxwellian spectrum are shown. The computed value of χ^2 per degree of freedom for this previously determined spectrum is 1.922. The mean and mean-square energies are given by Eqs. (7) and (8), and are listed in Table I together with other properties of the NBS spectrum.

Figures 1 and 2 both indicate that the NBS spectrum agrees with the experimental reference spectrum in the high energy region better than the least-squares adjusted Maxwellian spectrum. On the other hand, the NBS spectrum lies about 5-15% above experiment at energies below 0.5 MeV, giving rise to the factor of 2 deterioration in the value of χ^2 per degree of freedom relative to that of the least-squares adjusted Maxwellian spectrum. In the region between 0.8 and 3.0 MeV, the NBS and adjusted Maxwellian spectra behave similarly, with departures from experiment ranging from 1 to 5%. Neither representation reproduces the structure in the experimental spectrum between 1.5 and 3.0 MeV.

C. Los Alamos Spectrum.

The least-squares adjustment of the Los Alamos spectrum to the experimental differential spectrum is performed with respect to the nuclear level-density parameter a. As before, to obtain an absolute value of χ^2 per degree of freedom, the normalization of the experiment is recomputed for each iteration in the value of a. We find a minimum in χ^2, $\chi^2(\text{min}) = 0.552$, at a value of $a = A/9.15$ (MeV). This result yields the value of T_m from Eq. (20). The values of

measurements carried out by Grundl et al.[8] and Kobayashi et al.[9,10] We also compare the trends of each of the three sets of calculated integral cross sections to assess the overall quality of the three spectrum representations being used. This latter comparison is, of course, only possible if identical pointwise cross sections are used in each set of calculations.

The integral cross section $\langle\sigma_r\rangle$ representing the net effect of the pointwise cross section $\sigma_r(E)$ in the presence of the neutron field N(E) is given by

$$\langle\sigma_r\rangle = \frac{\int_{E_1}^{E_2} \sigma_r(E)\, N(E)dE}{\int_{E_1}^{E_2} N(E)dE}, \tag{23}$$

where E is the neutron energy, and E_1 and E_2 are the energy limits of the neutron field N(E). In this equation, $\sigma_r(E)$ is obtained from ENDF/B-V[23,24] with one exception,[25] and N(E) is one of the three spectrum representations that we are comparing. By choosing ENDF/B-V cross sections, the values of E_1 and E_2 are set at 10^{-5} eV and 20 MeV, respectively. A trapezoidal integration of Eq. (23) is performed for each reaction studied.

For purposes of graphical presentation and discussion of our results, we define an effective threshold energy, E_{th}, for each reaction studied, as the energy that divides the pointwise cross section integral at 0.01% and 99.99%. We use the ratio C/E of calculated integral cross sections to experimental integral cross sections as a function of E_{th} in the graphical presentation of our results that we now discuss.

A. Maxwellian Spectrum.

Our results for the least-squares adjusted Maxwellian spectrum are given in the fourth column of Table II where they can be compared directly with the experimental results in the third column, and in Fig. 5 where the C/E values are plotted as a function of the threshold energy E_{th}. There are three points to mention. First, Table II shows that for a given set of pointwise cross sections and the Maxwellian spectrum, seven of the fifteen calculations are outside of the two-sigma measurement uncertainty. Second, Fig. 5 shows that nine of the fifteen calculations are outside of the one-sigma measurement uncertainty. Third, the trend of the C/E ratios shown in Fig. 5 indicates that the

accuracy of the Maxwellian spectrum is increasingly worse with increasing reaction threshold. That is, the Maxwellian spectrum is too large (hard) in the high energy portion of the spectrum. This result is consistent with our conclusions for the differential spectrum comparisons of Sec. III. As already discussed in Secs. II.A. and III.A, this illustrates a fundamental difficulty in accounting for two physical effects with a single parameter.

B. NBS Spectrum.

Our results for the NBS spectrum are given in the fifth column of Table II and are illustrated in Fig. 6. Again, there are three points to be made. First, Table II shows for the identical set of pointwise cross sections and the NBS spectrum, only four of fifteen calculations are outside of the two-sigma measurement uncertainty. Second, Fig. 6 shows that only seven of the fifteen calculations are outside of the one-sigma measurement uncertainty. Third, the trend of the C/E ratios shown in Fig. 6 indicates that the NBS spectrum reproduces the experimental integral cross sections reasonably well for most values of the threshold energy.

C. Los Alamos Spectrum.

Our results for the Los Alamos spectrum are given in the last column of Table II and are illustrated in Fig. 7. Once again, there are three points to address. First, Table II shows that for the identical set of pointwise cross sections and the Los Alamos spectrum, only two of the fifteen calculations are outside of the two-sigma measurement uncertainty. Second, Fig. 7 shows that nine of the fifteen calculations are outside of the one-sigma measurement uncertainty. Third, the trend of the C/E ratios shown in Fig. 7 indicates that the Los Alamos spectrum, like the NBS spectrum, reproduces the experimental integral cross sections reasonably well for most values of the threshold energy.

To conclude this section, we combine Figs. 5-7 into Fig. 8, to provide a comparison of the trends of the C/E values with E_{th} for the three spectrum representations compared. For visual clarity we delete the experimental uncertainties. This figure clearly shows that the least-squares adjusted Maxwellian spectrum is unsatisfactory when using the present choice of the Poenitz and Tamura experiment to determine the Maxwellian temperature T_M = 1.429 MeV. Although we do not show the results here, this same conclusion is obtained when

using the popular value T_M = 1.42 MeV. Finally, the figure also indicates, on the basis of the chosen set of experimental integral cross sections, that the NBS and Los Alamos spectra could each be adjusted somewhat, were it not for the constraints imposed by the experimental differential spectrum measurements.

V. CONCLUSIONS

On the basis of the comparisons presented here, we conclude that the Los Alamos spectrum is the perferred representation of N(E) because it best reproduces both the differential and integral measurements, assuming ENDF/B-V cross sections in the calculation of the latter. Although the NBS spectrum reproduces the integral measurements fairly well, it fails to satisfactorily reproduce the recent differential measurements, and the Maxwellian spectrum fails to satisfactorily reproduce the recent integral measurements. Additionally, we calculate a value of $\bar{\nu}_p$ from the Los Alamos theory that is within approximately 1% of experiment. In this study we have learned that well-measured high-threshold integral cross sections provide valuable constraints on the differential spectrum, assuming the pointwise cross sections are well known. Finally, we mention that the Los Alamos spectrum has been adopted as the preliminary standard spectrum for ENDF/B-VI. The spectrum is available in tabular form from the U.S. National Nuclear Data Center, Brookhaven National Laboratory.

ACKNOWLEDGMENTS

We are grateful to W. P. Poenitz and K. Kobayashi for the use of their experimental data and for several stimulating discussions and communications. This work was supported by the U.S. Department of Energy.

REFERENCES

1. J. A. Grundl and C. M. Eisenhauer, in Proc. Conf. on Nuclear Cross Sections and Technology, Washington, D.C., March 3-7, 1975, Vol. I, p. 250, National Bureau of Standards Special Publication 425, Washington, D.C. (1975).

2. J. Grundl and C. Eisenhauer, in Proc. First ASTM-EURATOM Symp. on Reactor Dosimetry, Petten, Holland, September 22-26, 1975, Part I, p. 425, Commission of the European Communities, EUR 5667 e/f (1977).

3. D. G. Madland and J. R. Nix, Nucl. Sci. Eng. 81, 213 (1982).

4. D. G. Madland and J. R. Nix, in Proc. Conf. on Nuclear Data for Science and Technology, Antwerp, Belgium, September 6-10, 1982, p. 473, D. Reidel, Dordrecht (1983).

5. D. G. Madland and J. R. Nix, in Proc. Specialists' Meeting on Yields and Decay Data of Fission Product Nuclides, Brookhaven National Laboratory, Upton, New York, October 24-27, 1983, p. 423, Brookhaven National Laboratory publication BNL-51778 (1984).

6. W. P. Poenitz and T. Tamura, in Proc. Conf. on Nuclear Data for Science and Technology, Antwerp, Belgium, September 6-10, 1982, p. 465, D. Reidel, Dordrecht (1983).

7. W. P. Poenitz, private communication (April 1983).

8. H. T. Heaton II, D. M. Gilliam, V. Spiegel, C. Eisenhauer, and J. A. Grundl, in Proc. NEANDC/NEACRP Specialist Meeting on Fast Neutron Cross Sections of U-233, U-235, U-238, and Pu-239, Argonne National Laboratory, Argonne, Illinois, June 28-30, 1976, p. 333, Argonne National Laboratory publication ANL-76-90 (1976); update by J. Grundl, D. Gilliam, D. McHarry, C. Eisenhauer, and P. Soran, in memorandum to CSEWG Subcommittee on Standards (May 1982).

9. K. Kobayashi, I. Kimura, and W. Mannhart, J. Nucl. Sci. Tech. 19, 341 (1982).

10. K. Kobayashi, I. Kimura, H. Gotoh, and H. Tominaga, submitted to Ann. Repts. of the Res. Reactor Inst., Kyoto Univ. (July 1984).

11. F. D. Becchetti, Jr., and G. W. Greenless, Phys. Rev. 182, 1190 (1969).

12. J. P. Unik, J. E. Gindler, L. E. Glendenin, K. F. Flynn, A. Gorski, and R. K. Sjoblom, in Proc. Third IAEA Symp. on Physics and Chemistry of Fission, Rochester, New York, August 13-17, 1973, Vol. II, p. 19, International Atomic Energy Agency, Vienna (1974).

13. J. Terrell, Phys. Rev. 113, 527 (1959).

14. A. H. Wapstra and K. Bos, private communication to the National Nuclear Data Center, Brookhaven National Laboratory (March 1982).

15. P. Möller and J. R. Nix, At. Data Nucl. Data Tables 26, 165 (1981).

16. J. Weber, H. C. Britt, and J. B. Wilhelmy, Phys. Rev. C 23, 2100 (1981).

17. A. C. Wahl, J. Radioanalytical Chem. 55, 111 (1980).

18. D. G. Madland and R. J. LaBauve, Trans. Am. Nucl. Soc. 46, 760 (1984).

19. F. Pleasonton, R. L. Ferguson, and H. W. Schmitt, private communication (April 1982).

20. S. Amiel, in Proc. Second IAEA Symp. on Physics and Chemistry of Fission, Vienna, Austria, July 28-August 1, 1969, p. 569, International Atomic Energy Agency, Vienna (1969).

21. J. R. Smith, in Proc. Symp. on Nuclear Data Problems for Thermal Reactor Applications, Brookhaven National Laboratory, 1978, p. 5-1, Electric Power Research Institute publication EPRI-NP-1093 (1979).

22. R. R. Spencer, R. Gwin, and R. Ingle, Nucl. Sci. Eng. 80, 603 (1982).

23. B. A. Magurno, in Proc. Advisory Group Meeting on Nuclear Data for Reactor Dosimetry, Vienna, Austria, November 13-17, 1978, p. 1, International Atomic Energy Agency publication INDC(NDS)-103/M, Vienna (May 19[illegible]).

24. M. R. Bhat, in ENDF/B Summary Documentation, Brookhaven National Laboratory publication BNL-NCS-17541 (ENDF-201), Brookhaven National Laboratory (July 1979).

25. D. L. Smith, J. W. Meadows, and I. Kanno, Argonne National Laboratory report ANL/NDM-85, Argonne National Laboratory (June 1984).

TABLE I

SOME PROPERTIES OF THREE REPRESENTATIONS OF
THE PROMPT NEUTRON SPECTRUM FOR THE SPONTANEOUS FISSION OF ^{252}Cf

Quantity	Maxwellian	NBS	Los Alamos
Physical shape	smooth	five-segment piecewise continuous	smooth
Number of explicit parameters	1	12	3
Number of least-squares adjusted parameters in the present work	1	0	1
Adjusted Maxwellian temperature T_M (MeV)	1.429	—	—
Adjusted nuclear level-density parameter a (1/MeV)	—	—	A/9.15
$\langle E \rangle$ (MeV)	2.144	2.120	2.134
$\langle E^2 \rangle$ (MeV^2)	7.658	7.433	7.364
$\bar{\nu}_p$	—	—	3.810
χ^2 (min)	1.201	1.922[a]	0.552

[a] In this case, χ^2 (min) is the only value of χ^2 and it is calculated assuming zero degrees of freedom.

TABLE II

COMPARISON OF MEASURED AND CALCULATED INTEGRAL CROSS SECTIONS FOR THREE REPRESENTATIONS OF THE PROMPT NEUTRON SPECTRUM FOR THE SPONTANEOUS FISSION OF ^{252}Cf†

Reaction	E_{th} (MeV)	Measurement[a]	Maxwellian Calc.	(C/E)	NBS Calc.	(C/E)	Los Alamos Calc.	(C/E)
$^{235}U(n,f)$	0.00	1216.0 ± 19.46	1238.657	(1.019)	1235.918	(1.016)	1235.720	(1.016)
$^{115}In(n,n')$	0.76	201.0 ± 8.2	182.804	(0.909)*	181.936	(0.905)*	186.009	(0.925)
$^{58}Ni(n,p)$	0.80	118.5 ± 4.1	115.888	(0.978)	113.891	(0.961)	114.039	(0.962)
$^{47}Ti(n,p)$	1.14	21.58 ± 1.16	24.463	(1.134)*	24.070	(1.115)*	24.209	(1.122)*
$^{54}Fe(n,p)$	1.36	87.63 ± 4.35	89.968	(1.027)	88.346	(1.008)	88.323	(1.008)
$^{32}S(n,p)$	1.80	72.52 ± 2.96	72.665	(1.002)	71.447	(0.985)	71.662	(0.988)
$^{27}Al(n,p)$	2.86	4.891 ± 0.179	5.375	(1.099)*	5.140	(1.051)	4.967	(1.016)
$^{46}Ti(n,p)$	2.97	14.04 ± 0.61	14.080	(1.003)	13.474	(0.960)	13.014	(0.927)
$^{51}V(n,p)$[b]	3.41	0.713 ± 0.059	0.732	(1.027)	0.688	(0.966)	0.657	(0.921)
$^{56}Fe(n,p)$	4.65	1.440 ± 0.070	1.546	(1.073)	1.416	(0.983)	1.322	(0.918)
$^{48}Ti(n,p)$	5.07	0.415 ± 0.016	0.460	(1.107)*	0.410	(0.986)	0.377	(0.907)*
$^{59}Co(n,\alpha)$	5.52	0.218 ± 0.014	0.243	(1.115)	0.217	(0.997)	0.200	(0.919)
$^{24}Mg(n,p)$	5.58	1.940 ± 0.093	2.404	(1.239)*	2.159	(1.113)*	1.995	(1.028)
$^{27}Al(n,\alpha)$	5.71	1.006 ± 0.022	1.195	(1.187)*	1.060	(1.053)*	0.973	(0.967)
$^{197}Au(n,2n)$	8.31	5.267 ± 0.226	6.817	(1.294)*	5.650	(1.073)	4.973	(0.944)

† Using ENDF/B-V pointwise cross sections, unless otherwise noted, and expressing the results in millibarns.

* Calculation outside two-sigma measurement uncertainty.

[a] The experimental measurements are those of Grundl et al. (Ref. 8) and Kobayashi et al. (Refs. 9 and 10).

[b] The pointwise cross section used in the calculation for this reaction is from Smith et al. (Ref. 25).

FIGURE CAPTIONS

Fig. 1. Prompt fission neutron spectrum in the laboratory system for the spontaneous fission of ^{252}Cf. The dashed curve gives the least-squares adjusted Maxwellian spectrum calculated with Eq. (1), the dot-dashed curve gives the NBS spectrum calculated with Eq. (4), and the solid curve gives the least-squares adjusted Los Alamos spectrum calculated with Eq. (9). The experimental data are those of Poenitz and Tamura (Refs. 6 and 7).

Fig. 2. Ratio of the NBS spectrum and the experimental spectrum to the least-squares adjusted Maxwellian spectrum, corresponding to the curves shown in Fig. 1.

Fig. 3. Ratio of the least-squares adjusted Los Alamos spectrum and the experimental spectrum to the least-squres adjusted Maxwellian spectrum, corresponding to the curves shown in Fig. 1.

Fig. 4. Ratio of the NBS spectrum, the least-squares adjusted Los Alamos spectrum, and the experimental spectrum to the least-squares adjusted Maxwellian spectrum, corresponding to the curves shown in Fig. 1.

Fig. 5. Ratio of calculated to experimental integral cross sections for the prompt neutron spectrum from the spontaneous fission of ^{252}Cf as a function of the effective neutron threshold energy for the reaction. The calculated values are obtained using the least-squares adjusted Maxwellian spectrum from Eq. (1) in Eq. (23) together with ENDF/B-V pointwise cross sections. The experimental values are those of Grundl et al. (Ref. 8) and Kobayashi et al. (Refs. 9 and 10). The error bars shown are due only to the experimental uncertainties. The dashed line serves as a guide to the eye.

Fig. 6. Similar to Fig. 5 except that the calculated integral cross sections are obtained using the NBS spectrum from Eq. (4). The dot-dashed line serves as a guide to the eye.

Fig. 7. Similar to Fig. 5 except that the calculated integral cross sections are obtained using the least-squares adjusted Los Alamos spectrum from Eq. (9). The solid line serves as a guide to the eye.

Fig. 8. Comparisons of ratios of calculated to experimental integral cross sections shown in Figs. 5-7 with error bars deleted for clarity. The dashed, dot-dashed, and solid lines serve as guides to the eye.

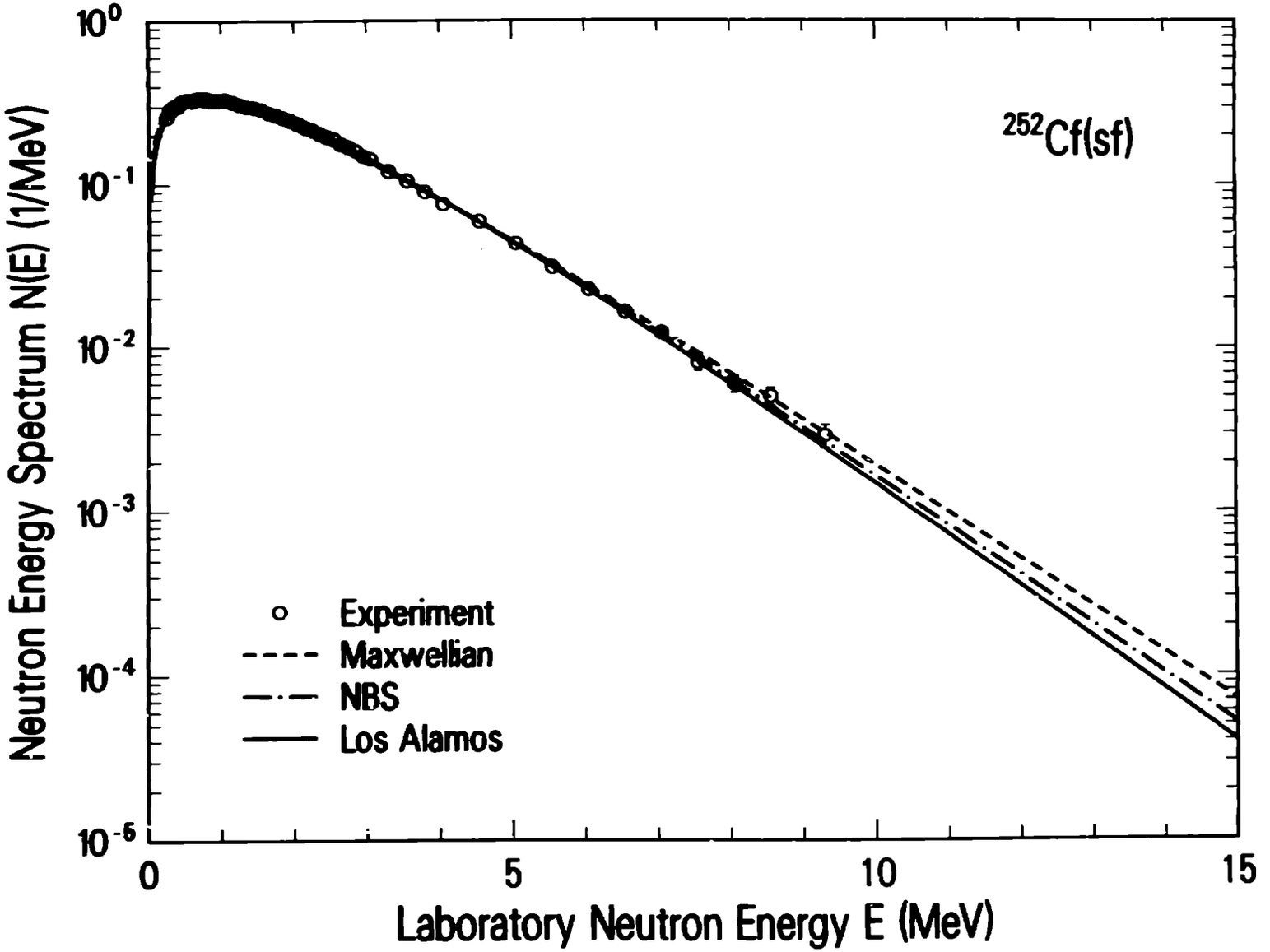
10^0
10^{-1}
10^{-2}
10^{-3}
10^{-4}
10^{-5}
Neutron Energy Spectrum N(E) (1/MeV)
^{252}Cf(sf)
Experiment
Maxwellian
NBS
Los Alamos
0
5
10
15
Laboratory Neutron Energy E (MeV)

Figure 1.

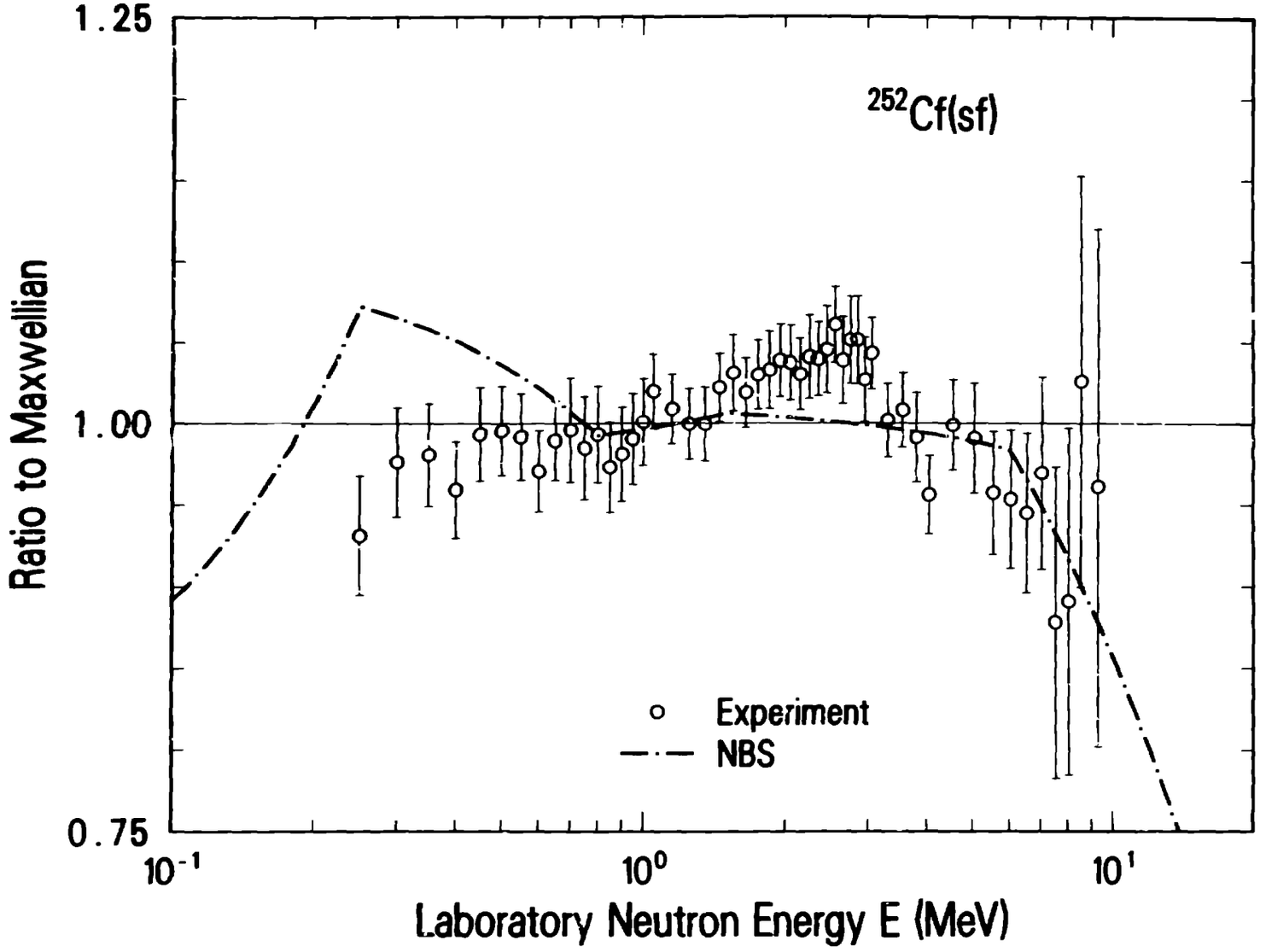
1.25
1.00
0.75
Ratio to Maxwellian
252Cf(sf)
Experiment
NBS
10-1
100
101
Laboratory Neutron Energy E (MeV)

Figure 2.

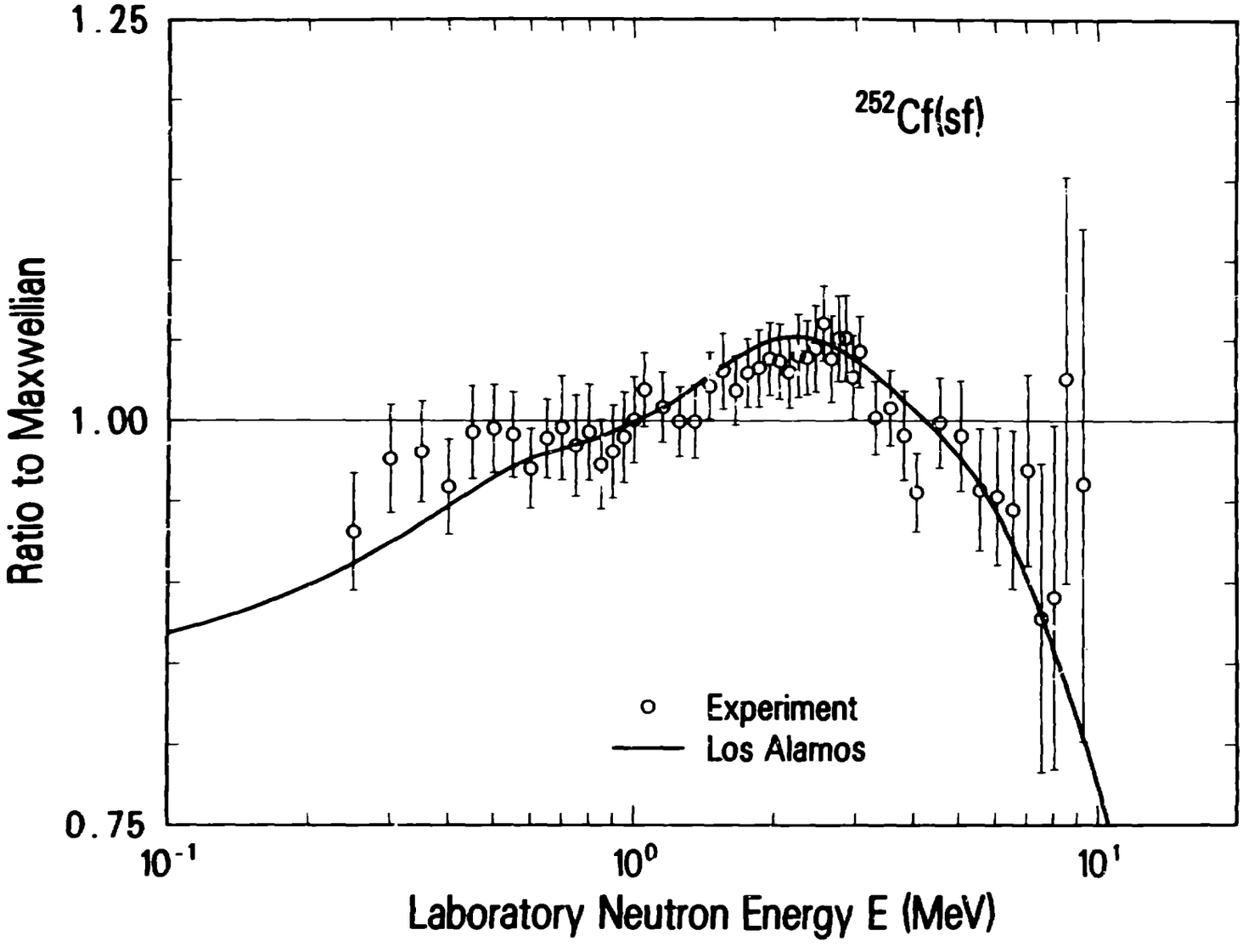
1.25
1.00
0.75
Ratio to Maxwellian
252Cf(sf)
Experiment
Los Alamos
10-1
100
101
Laboratory Neutron Energy E (MeV)

Figure 3.

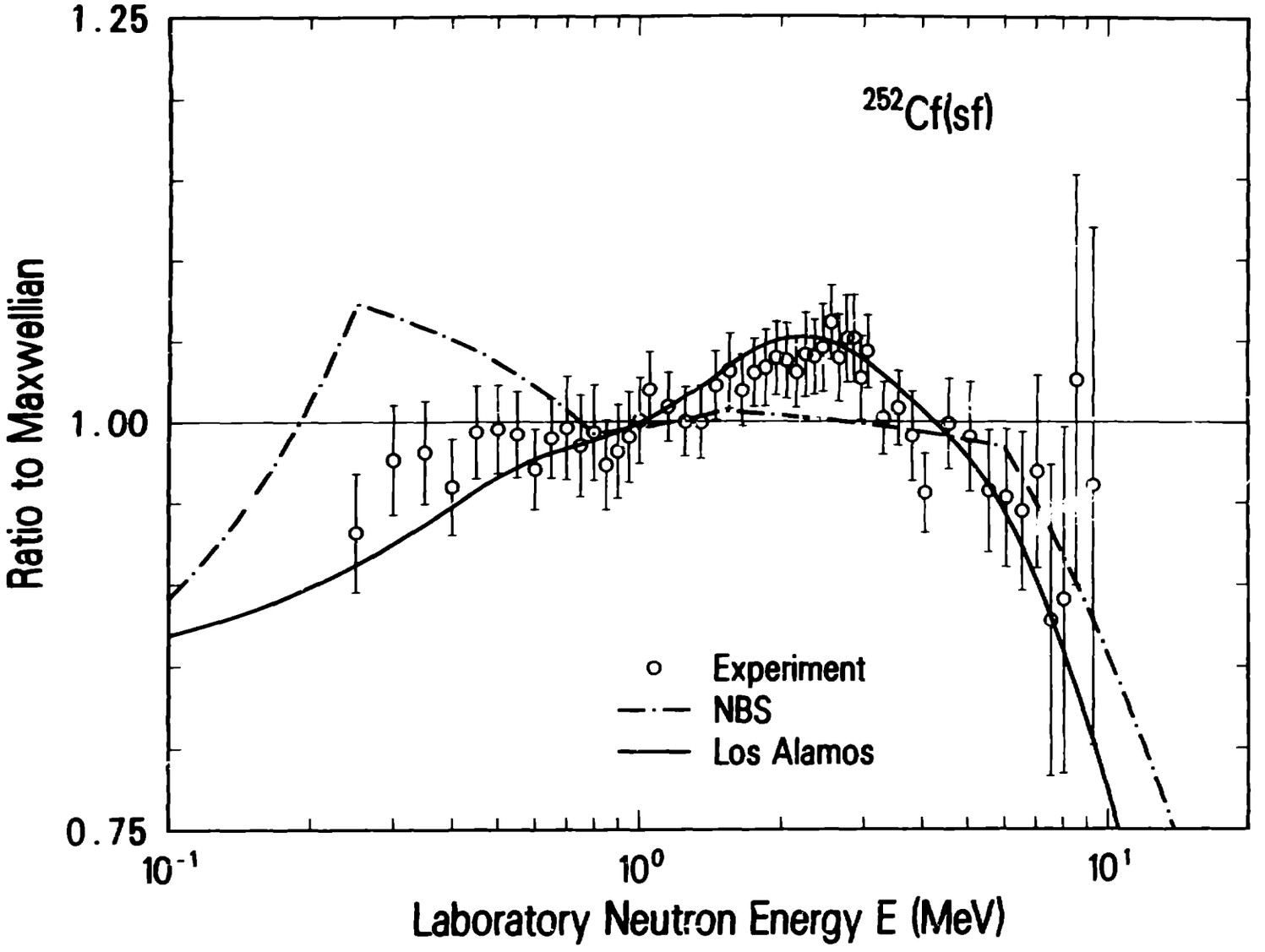
1.25
1.00
0.75
Ratio to Maxwellian
^{252}Cf(sf)
Experiment
NBS
Los Alamos
10^{-1}
10^{0}
10^{1}
Laboratory Neutron Energy E (MeV)

Figure 4.

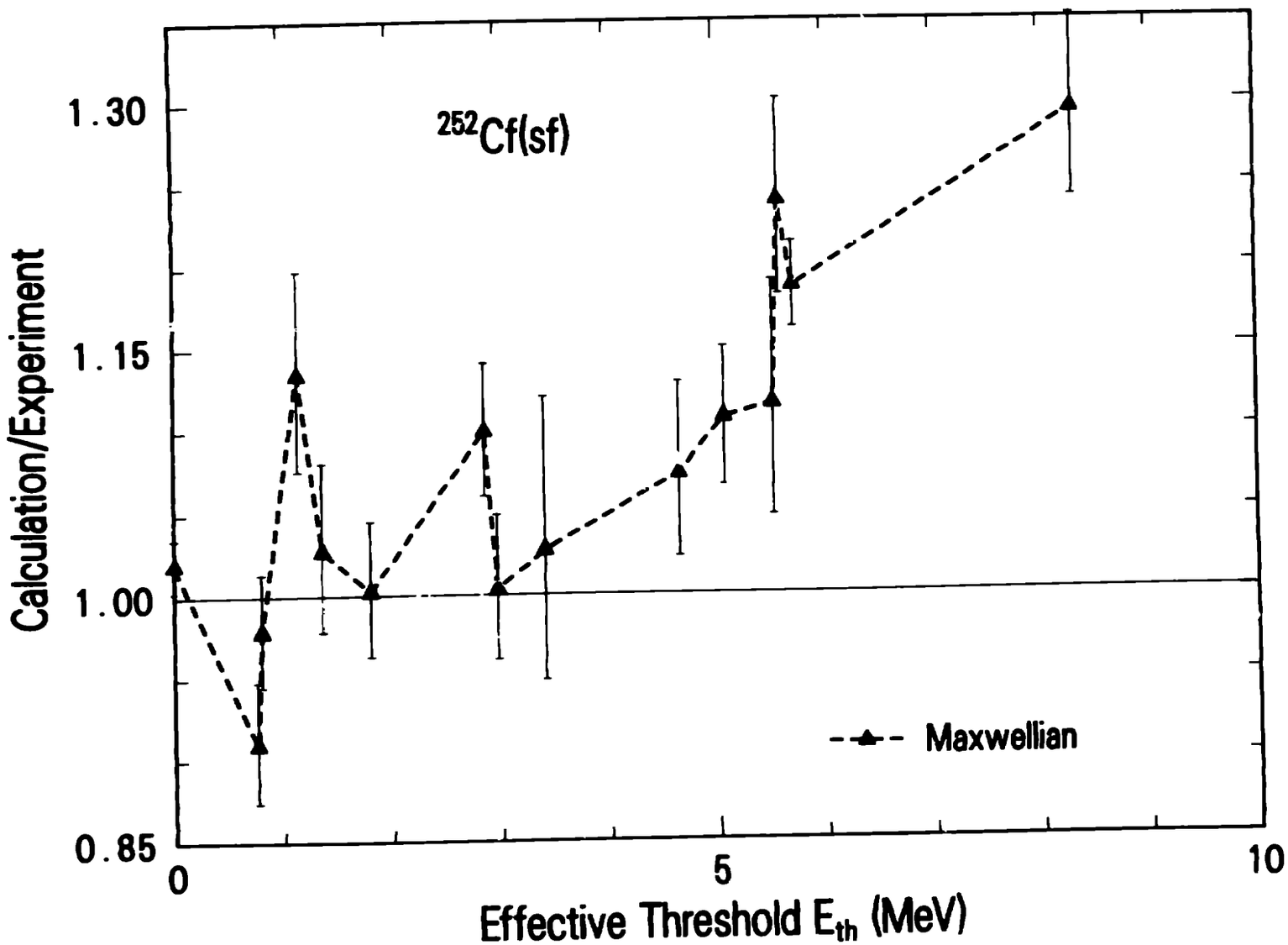
252Cf(sf)
1.30
1.15
1.00
0.85
Calculation/Experiment
0
5
10
Effective Threshold Eth (MeV)
Maxwellian

Figure 5.

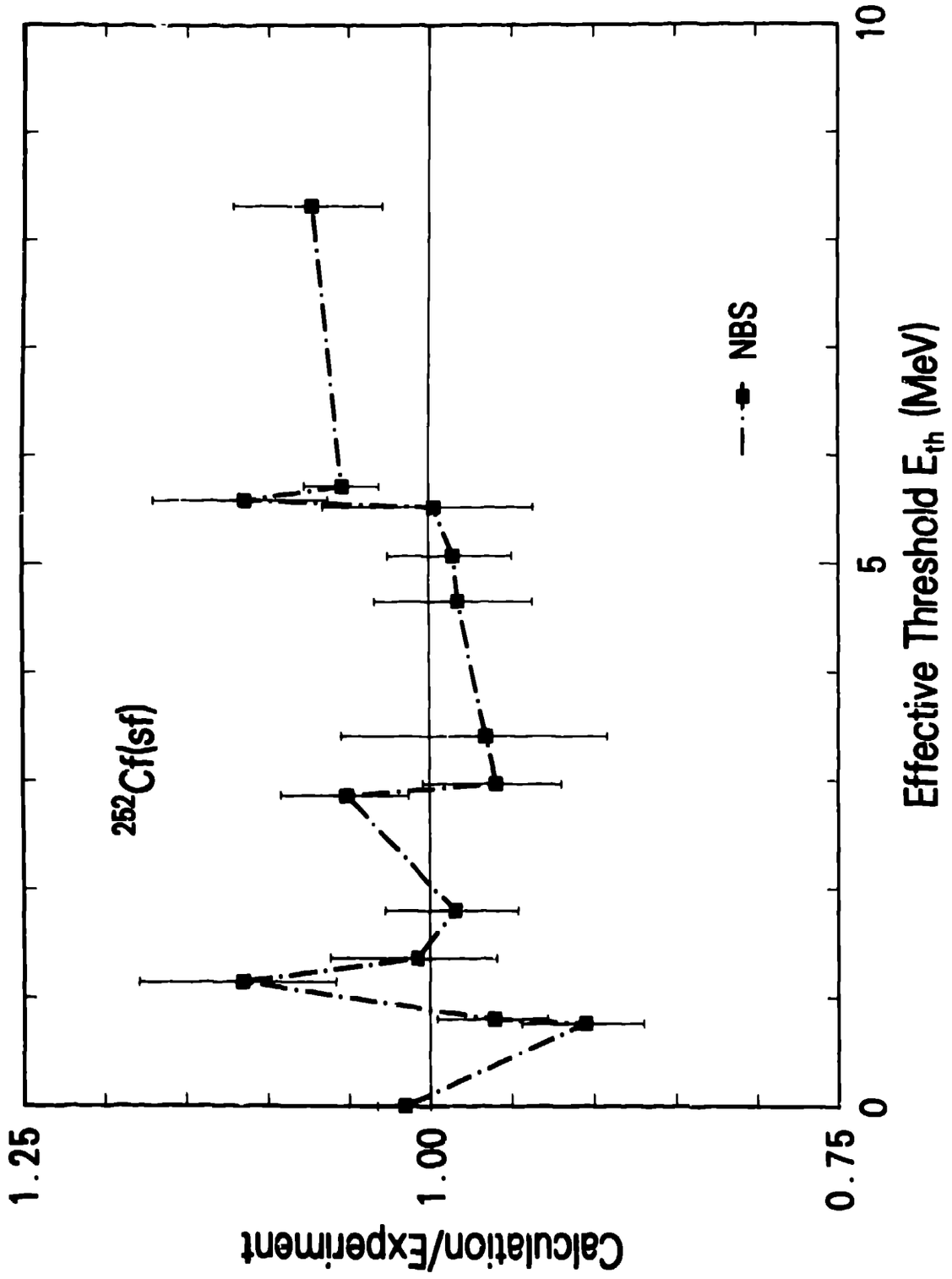
Calculation/Experiment
1.25
1.00
0.75
0
5
10
Effective Threshold E_{th} (MeV)
^{252}Cf(sf)
NBS

Figure 6.

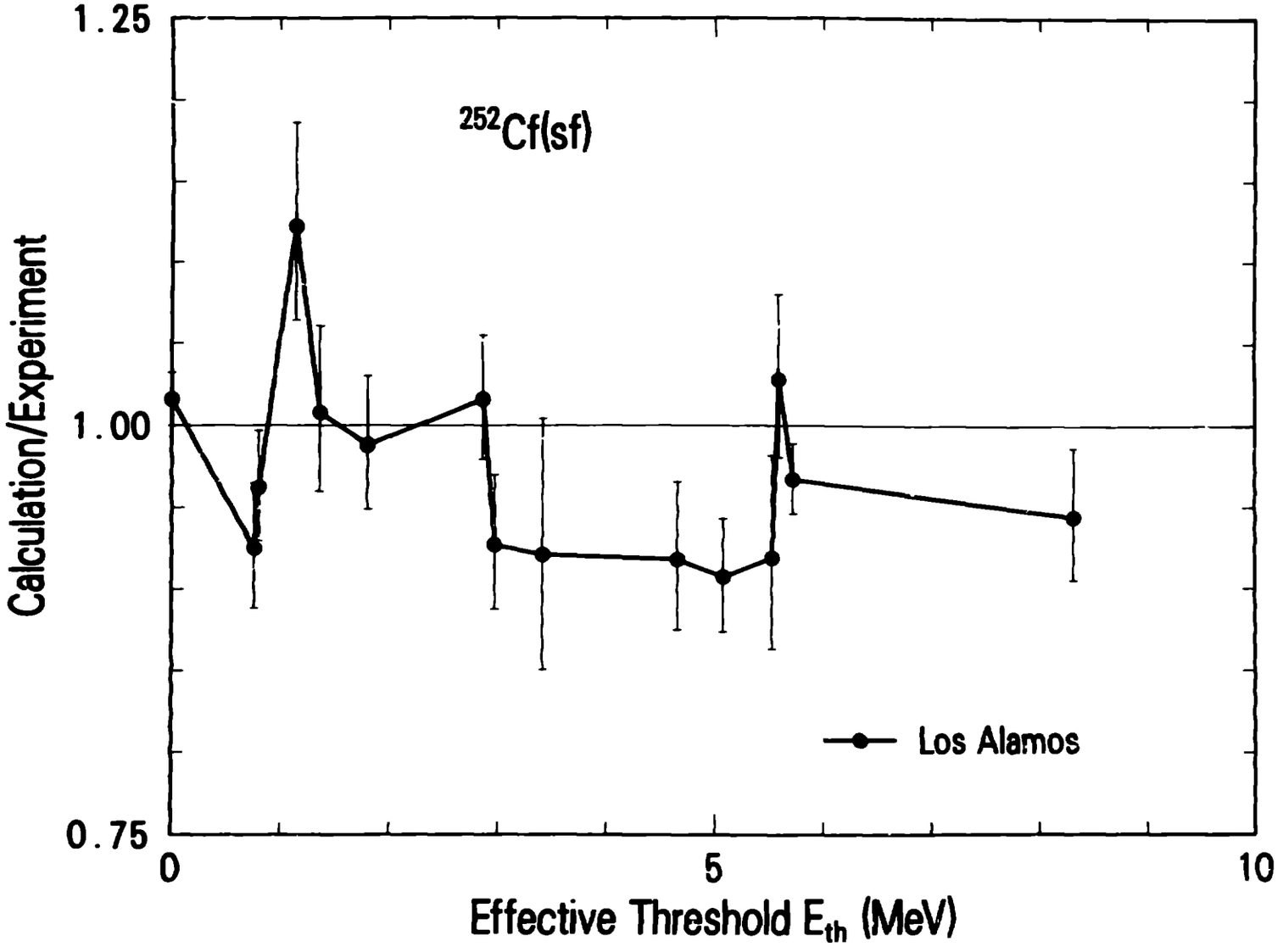
1.25
1.00
0.75
Calculation/Experiment
^{252}Cf(sf)
Los Alamos
0
5
10
Effective Threshold E_{th} (MeV)

Figure 7.

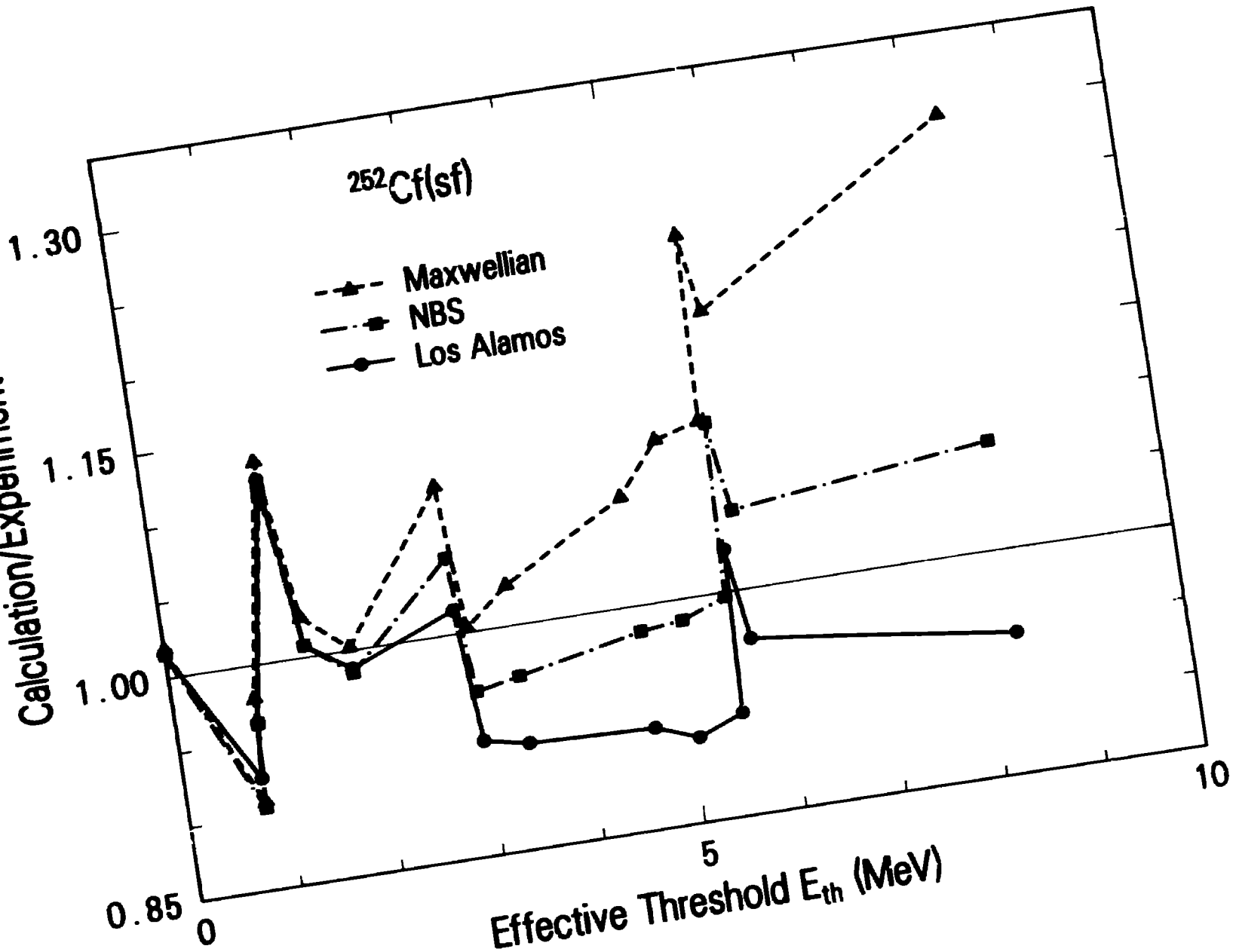
^{252}Cf(sf)
Maxwellian
NBS
Los Alamos
Calculation/Experiment
1.30
1.15
1.00
0.85
0
5
10
Effective Threshold E_{th} (MeV)

Figure 8.